Available online at www.sciencedirect.com
ScienceDirect
Catalysis Today 117 (2006) 454–461
CATALYSIS TODAY
www.elsevier.com/locate/cattod

Rh–La(Mn,Co)O_3 monolithic catalysts for the combustion of methane under fuel-rich conditions

S. Cimino [a,*], G. Landi [b], L. Lisi [a], G. Russo [a]

[a] *Istituto di Ricerche sulla Combustione, CNR, Napoli, Italy*
[b] *Dipartimento di Ingegneria Chimica, Università Federico II, Napoli, Italy*

Available online 31 July 2006

Abstract

Novel Rh–La(Mn,Co)O_3 structured catalysts were developed for the partial oxidation of methane to syngas intended as a preliminary conversion step in combustion systems such as power turbines and utility burners employing a fuel-rich fuel-lean approach to reduce NO_x formation. Active components were impregnated on La–γ-Al_2O_3 washcoated honeycomb monoliths and the catalysts were characterised by BET, SEM/EDS, H_2-TPR, and in situ FT-IR under reaction conditions. Catalytic partial oxidation of methane was tested under both pseudo-isothermal and pseudo-adiabatic conditions showing that the process can be conducted with high yield and selectivity: improved and stable performances were found especially in the case of Rh–$LaMnO_3$ catalyst, due to the synergism between active sites and to the stabilization of the noble metal.

Keywords: Catalytic combustion; Catalytic partial oxidation; Natural gas; Syngas; Rh–perovskite; Structured catalyst

1. Introduction

Ultra low emissions catalytic combustion of methane under fuel-lean conditions is generally carried out over Pd based catalysts. Nevertheless, deactivation at high temperature, occurrence of large activity hysteresis cycles and strong oscillating behaviours require to limit the catalyst temperature and represent a serious limit to practical implementation of this technology [1]. Fuel-rich catalytic combustion has been recently proposed as a preliminary conversion stage for gas turbine burners. In this process, a fuel-rich/air mixture is catalytically converted to both partial and total oxidation products that are subsequently oxidized with excess air to complete the combustion in a homogeneous flame [2]. The presence of syngas in the hot product stream from the catalytic zone can help in stabilizing lower temperature flames in the burnout zone, thus reducing NO_x emissions [3]. The limited extent of the catalytic reaction, due to the poor oxygen availability, prevents the catalyst from reaching high temperatures even in the presence of a not perfectly mixed feed, thus avoiding catalyst deactivation and significantly improving its durability [2]. Moreover, the absence of adsorbed surface oxygen under fuel-rich conditions minimizes catalyst volatilization as noble metal oxide [2].

It has been demonstrated that catalytic partial oxidation of methane can yield near complete conversion to mostly H_2 and CO at millisecond contact times in structured catalytic reactors running autothermally, entailing dramatic reduction in reactor size and complexity [4–6]. Several studies have reported that catalysts with high Rh loadings (5–15%, w/w) onto ceramic foam monoliths and honeycombs provided the best performances compared to Pd and Pt based systems in terms of light off temperature, H_2 yields, stability against volatilization, resistance to carbon deposition [2,4,5]. On the other hand, few studies have focused on the influence of support material and its interactions with the noble metal, especially under operating conditions of interest for industrial application [7,8]. In particular, it was reported that irreducible oxides promote the formation of active Rh metal sites more than reducible supports [9] and that the use of hexaaluminates as Rh supports resulted in lower syngas yield and lower stability than α-Al_2O_3 [10]. On the other hand, we have recently found that the strong synergy and interaction existing between noble metals (Pt, Pd) and a perovskite support ($LaMnO_3$) led to enhanced catalyst performance in terms of activity and stability at high operating temperature both in the lean

* Corresponding author. Tel.: +39 081 7682233; fax: +39 081 5936936.
E-mail address: stcimino@unina.it (S. Cimino).

0920-5861/$ – see front matter
doi:10.1016/j.cattod.2006.06.016

catalytic combustion and the oxidative dehydrogenation of light hydrocarbons [11,12]. In fact, the addition of Rh to a perovskite phase has been proposed in order to better disperse the noble metal, thus reducing its required amount, and to stabilize it in a wider range of temperatures [13–15]. Moreover, the simultaneous presence of total oxidation and reforming active sites in the same catalytic system is expected to reduce light off temperature, enhance methane conversion and inhibit coke formation. On such a basis, in this work Rh–$La(Mn,Co)O_3$ alumina supported structured catalysts have been developed and tested for the oxidation of methane/air mixtures under fuel-rich conditions.

2. Experimental

2.1. Catalyst preparation and characterisation

Commercial cordierite monoliths (Corning) with a cell density of 400 or 600 cpsi were coated using a modified dip-coating procedure with a thick La_2O_3 (∼7%, w/w)-stabilised γ-Al_2O_3 layer and calcined in air at 800 °C. Rh and perovskite precursors were deposed on the stabilised alumina washcoat through impregnation with an aqueous solution (0.23 M) of $La(NO_3)_3{\cdot}6H_2O$ (Aldrich, >99.99%) and $Co(NO_3)_2{\cdot}4H_2O$ (Aldrich, >99%) or $(CH_3CO_2)_2Mn{\cdot}4H_2O$ (Aldrich, >99%) and $Rh(NO_3)_2{\cdot}2H_2O$ (Fluka, purum) (0.027 M). Reference monolith samples with the same amount of Rh but without perovskite phase were also prepared. The samples were dried in MW oven and in stove at 120 °C and calcined at 800 °C for 3 h under flowing air. The process was repeated 10 times in order to achieve the target loading (∼30%, w/w perovskite and 1%, w/w Rh with respect to the active washcoat layer, monolithic substrate excluded). In the following, catalysts containing Co will be quoted as LCR, while those containing Mn will be labelled as LMR.

The BET specific surface area of monolith samples, evaluated by N_2 adsorption at 77 K using a Carlo Erba 1900 Sorptomatic apparatus after degassing under vacuum at 200 °C, was assigned only to the active washcoat layer (SSA of cordierite substrate ≤ 1 m^2/g). Morphological characterisation was performed using a Philips XL30 Scanning Electron Microscope equipped with an EDAX detector for EDS microanalysis.

TPR and FT-IR measurements were performed on reference powder catalysts with same composition (named Rh–$LaCoO_3$/Al_2O_3, Rh–$LaMnO_3$/Al_2O_3) which were prepared by repeated incipient wetness impregnations of the La-stabilised alumina powder used as washcoat for the monoliths. TPR experiments were carried out with Micrometrics TPD/TPR 2900 apparatus equipped with a TCD. The samples were pretreated at 800 °C under air flow for 1 h before the experiment, and then reduced with a 2% H_2/Ar mixture (25 cm^3 min^{-1}), heating 10 °C min^{-1} from RT up to 800 °C.

FT-IR spectra were recorded with a Perkin-Elmer Spectrum GX spectrometer with a spectral resolution of 4 cm^{-1} on catalyst pressed into self-supported disk in a IR cell equipped with a ZnSe window operating under gas flow up to 800 °C. CO was adsorbed feeding 100 cm^3 min^{-1} of 2% CO/N_2 mixture at room temperature for 30 min on the sample outgassed at 300 °C or pre-reduced at 300 °C with a 2% H_2/N_2 mixture. Spectra were also recorded under reaction conditions by feeding 100 cm^3 min^{-1} of a CH_4/O_2/Ar mixture (2/1/97) at 400, 550 and 700 °C, respectively.

2.2. Experimental set-up

Catalytic tests were carried out on monoliths in two ways:

- Pseudo-isothermally, to compare the intrinsic activity of the monolith catalysts under controlled fluid dynamics: 400 cpsi monoliths (with 8 out of 25 open channels on the section) were cut to a standard length of 35 mm and positioned inside quartz reactor (d = 10mm), externally heated by a three zone electrical tubular furnace. The central monolith channel was blocked for catalyst wall temperature measurement with two K-type thermocouples. Standard feed composition was $CH_4/O_2/N_2$ = 2/1.2/96.8, at GHSV 7×10^4 h^{-1} based on monolith volume.
- Pseudo-adiabatically, in order to reproduce conditions of practical interest, using 600 cpsi monoliths in the shape of disks (L = 11 mm, D = 17 mm) with a smaller external surface/volume ratio, which controls heat exchange with the surroundings. The catalytic monoliths were stacked between two inert radiation shields (mullite foams, 45 ppi) and tightly sealed in a quartz tube that was inserted in an electric furnace. Reactor temperatures were measured by means of thermocouples in the centre of each monolith, in close contact with the solid, and in the exit gas after the last radiation shield [12,15]. In these experiments the inlet CH_4/air mixture, without dilution and always above the upper flammability limit, was normally fed at GHSV 3.6×10^4 h^{-1}, corresponding to a residence time of roughly 25 ms at the average temperature of 900 °C.

Exit gases passed through a $CaCl_2$ trap to remove water, prior to splitting to a Hartmann & Braun Advance Optima continuous analyser for H_2, CO, CO_2, CH_4, and to an on line GC (HP5890 Series II). Carbon balance was always closed within ±4%. No other hydrocarbons except from methane were detected in the products, whereas O_2 was always completely converted.

3. Results and discussion

Table 1 reports catalysts denomination, loading of active washcoat and its nominal weight composition as well as measured specific surface areas. Specific surface area of active layer after repeated calcination at 800 °C was lowered to roughly 70 m^2/g compared to ∼200 m^2/g of the starting submicronic γ-Al_2O_3 powder, due to the introduction of the different active phases components, regardless of the type of transition metal cation in the perovskite.

SEM/EDS analysis showed a good adhesion of both support and active phase and a uniform distribution of La and transition

Table 1
Catalysts denomination, shape, active phase content, nominal composition and specific surface area

Catalyst	Number, density of cells (cpsi)	d_h (mm)	L (mm)	Active layer (g) (wt.%)	Nominal composition (wt.%)[a]			BET[a] (m^2/g)
					La/γ-Al_2O_3	La(Co,Mn)O_3	Rh	
LCR_1	25 (400)	1.09	35	0.49 (35.6)	67.50	31.45	1.05	69.7
LCR_2	210 (600)	0.96	11	0.94 (52.6)	69.50	29.52	0.98	69.2
LMR_1	25 (400)	1.09	36	0.46 (32.8)	68.11	30.91	0.98	70.2
LMR_2	210 (600)	0.96	11	0.91 (50.4)	69.95	29.1	0.95	68.4

[a] Referred to the weight of active layer, monolithic substrate excluded.

metal into the alumina washcoat, whereas Rh penetration was limited to a surface layer < 10 μm [15].

3.1. H_2-TPR and FT-IR experiments

Fig. 1 shows H_2-TPR profiles of the catalysts while Table 2 reports the results of the integration of total and partial (when peaks are completely resolved) TPR signals in terms of H_2 uptake and H_2/Me ratio, where Me is the reducible element present in the sample (noble or transition metal). For mixed samples Me should represent the sum of Rh and transition metal, however, the possible contribution of Rh has been neglected due to its relatively low atomic content (about 1/10th). In the absence of perovskite, rhodium undergoes reduction at very low temperature, showing a peak at 135 °C with a shoulder at 200 °C while a further reduction peak was detected at $T > 600$ °C. The low temperature peaks have been attributed to the reduction of RhO_x species weakly interacting with the support [16,17]. The high temperature signal has been associated [17] to the reduction of spinel type species $Rh(AlO_2)_y$, formed by reaction between alumina and noble metal at high temperature. The integration of all signals, reported in Table 2, provides a H_2/Rh ratio which is about 1/2 of theoretical value corresponding to the reduction of Rh^{3+} to metallic rhodium, suggesting that a fraction of Rh is not reducible or that in the fresh sample Rh has an average oxidation state lower than +3.

In the presence of perovskite the low temperature signal of rhodium disappears suggesting that the noble metal is involved in the formation of a solid solution with the perovskite

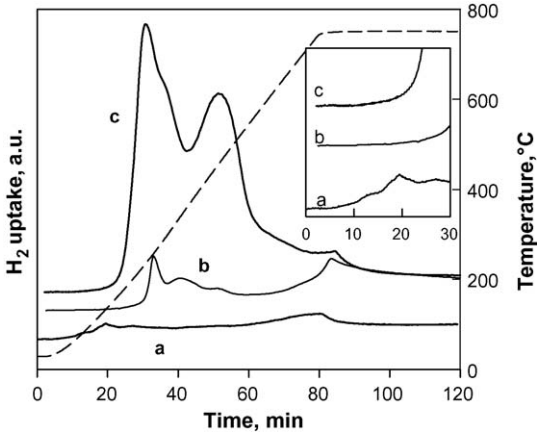

Fig. 1. TPR curves of (a) Rh/Al_2O_3, (b) $Rh–LaCoO_3/Al_2O_3$ and (c) $Rh–LaMnO_3/Al_2O_3$ catalysts.

modifying its redox behaviour. Reduction of rhodium at high temperature cannot be excluded, but it is hardly detectable due to the signal of perovskite in the same range of temperature [18,19]. TPR curve of $Rh–LaMnO_3/Al_2O_3$ shows two or more not resolved peaks with maxima at 232 and 455 °C, respectively, whose overall integration (Table 2) provides an H_2/Mn ratio = 0.8, higher than that required (0.5) for reduction of manganese from +3 to + 2. This led to roughly estimate a 60% fraction of Mn^{4+} in the fresh sample. In the case of bulk $LaMnO_3$ perovskite it has been reported the presence of significant fraction of Mn^{4+} [17–20], whose amount and redox properties can be affected by partial substitution with another cation in the B position [18,19] or by dispersion on a support [21]. Although it can be hypothesized that Rh substitution and/or $Rh–LaMnO_3$ dispersion on alumina contribute to increase the reducibility with respect to bulk $LaMnO_3$, it is possible that part of the Mn^{4+} detected is due the presence of single oxides such as MnO_2. In fact, the reduction of bulk MnO_2 occurs in two steps in the temperature range 250–400 °C [21].

On the other hand, a much lower reduction of cobalt with respect to that reported for bulk $LaCoO_3$ [19] was observed for $Rh–LaCoO_3/Al_2O_3$ sample, indicating that Co is involved in the formation of a $CoAl_2O_4$ spinel with alumina, as also suggested by the blue colour of the catalyst particle core. The low temperature signal is clearly consisting of two peaks, with maxima at 259 and 344 °C, likely attributable to the reduction of Co^{3+} to Co^{2+} and of Co^{2+} to Co^0, as observed for bulk $LaCoO_3$ [19], whereas the signal starting just before the isothermal step of the experiment can be attributed to the reduction of $CoAl_2O_4$ spinel and/or to that of $Rh(AlO_2)_y$.

In agreement with these results, FT-IR spectrum of CO adsorbed at room temperature on Rh/Al_2O_3 pre-reduced in situ under H_2 at 300 °C (Fig. 2b) shows the appearance of three bands at 2020, 2065 and 2100 cm^{-1}, not present for the fresh

Table 2
H_2 uptake and H_2/Me ratio evaluated from the integration of TPR signals (Me = Rh for Rh/Al_2O_3; Me = transition metal for $Rh–LaMO_3$)

Catalyst	H_2 uptake ($\times 10^3$ mol g^{-1})			H_2/Me
	First peak	Second peak	Total	
Rh/Al_2O_3	0.033	0.030	0.063	0.65
$Rh–LaCoO_3/Al_2O_3$	0.083	0.15	0.030	0.19
$Rh–LaMnO_3/Al_2O_3$	–	–	1.01	0.81

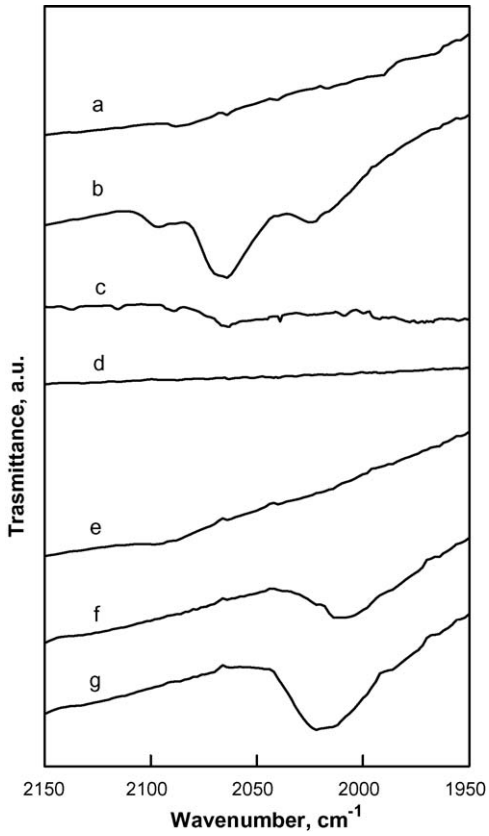

Fig. 2. FT-IR spectra after CO adsorption on: Rh/Al_2O_3 (a) evacuated at 300 °C and (b) pre-reduced with H_2 at 300 °C; (c) $Rh–LaMnO_3/Al_2O_3$ and (d) $Rh–LaCoO_3/Al_2O_3$ pre-reduced with H_2 at 300 °C. FT-IR spectra of Rh/Al_2O_3 under reaction mixture at (e) 400 °C, (f) 550 °C and (g) 700 °C.

catalyst (Fig. 2a), which confirm that rhodium oxide is easily reduced by H_2 at quite low temperature. Indeed, both 2020 and 2100 cm^{-1} signals have been attributed by Dulaurent et al. [22] to CO *gem*-dicarbonyl species and the one peaked at 2065 cm^{-1} to linear CO species [22,23] adsorbed on supported metal Rh. In contrast, only a very weak signal appears for $Rh–LaMnO_3/Al_2O_3$ at 2065 cm^{-1} (Fig. 2c), whereas no bands are present in this region for Co containing catalyst (Fig. 2d), thus confirming that reduction of rhodium to Rh^0 is totally (for $Rh–LaCoO_3/Al_2O_3$) or partially (for $Rh–LaMnO_3/Al_2O_3$) inhibited by the presence of the additional oxide phase. In fact, the absence of perovskite skeletal vibrations in the region above 1500 cm^{-1} for $Rh–LaCoO_3/Al_2O_3$, detected for Mn containing sample, indicates a significant formation of a perovskite-like phase only for the latter catalyst, which likely allows a small fraction of rhodium to preserve its original redox properties.

3.2. *In situ FT-IR under reaction*

FT-IR spectra were also recorded under reaction mixture at 400, 550 and 700 °C, in order to investigate on the possible reduction of rhodium induced by the methane partial oxidation reaction. The occurrence of the reaction was verified for all the tested catalysts by the decrease of methyl band and the appearance of that of gaseous CO. For Rh/Al_2O_3 sample a band centred at 2020 cm^{-1}, absent at 400 °C (Fig. 2e), appears at 550 °C (Fig. 2f) and further increases at 700 °C (Fig. 2g), shifting, at the same time, to lower frequencies; on the other hand no signals were detected for the two perovskite containing catalysts. This new band does not correspond to linear adsorbed CO on pre-reduced supported Rh and it cannot be associated to dicarbonyl species, since the other characteristic signal at 2100 cm^{-1} is missing. In fact it could suggests the formation of carbonyl hydride on metallic Rh, as found by Solymosi and Pásztor [23] on pre-reduced Rh/Al_2O_3 during the simultaneous adsorption of H_2 and CO_2.

In this case, the presence of H_2 produced by the reaction could promote the formation of Rh(HCO), whose amount increases with the reaction temperature due to the progressively

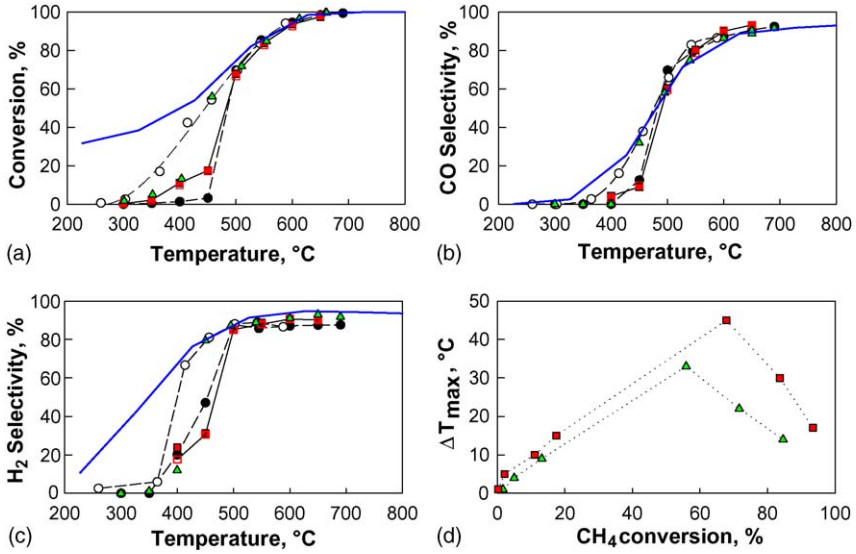

Fig. 3. CH_4 conversion, syngas selectivity and maximum temperature increase over the monolith as a function of preheating temperature for Rh/Al_2O_3 (●, ○), LMR_1 (■, □) and LCR_1 (▲) catalyst under pseudo-isothermal CPO tests; first heating, full symbols; subsequent cooling, open symbols. Solid lines correspond to equilibrium among gaseous species only.

higher concentrations of both H_2 and CO, and of metallic Rh centres that are able to adsorb them.

It must be underlined that the strong increase of the intensity of the signal at 2020 cm^{-1} with reaction temperature is in agreement with the steep increase of CH_4 conversion observed in the pseudo-isothermal catalytic tests starting from 500 °C (see Section 3.3), confirming that metallic rhodium is formed under reaction conditions and represents the active form of the noble metal.

As already pointed out, the reaction occurs in the same temperature range also on perovskite containing catalysts, but no signals were detected for both Rh–$LaCoO_3/Al_2O_3$ and Rh–$LaMnO_3/Al_2O_3$ under the same conditions. It is confirmed that the presence of perovskite oxide inhibits the formation of metallic rhodium, in agreement with results of TPR experiments, likely giving rise to a new mixed active phase.

3.3. Pseudo-isothermal catalytic tests

Under pseudo-isothermal conditions, Rh/Al_2O_3 monolith catalyst showed (Fig. 3) a steep increase of CH_4 conversion above 450 °C; for $T \geq 500$ °C methane conversion closely approached the equilibrium curve, which was estimated using CHEMKIN 4.0.1 software [24] among gaseous species only, after having ruled out C-formation on the catalyst. During the following cooling cycle higher conversions were obtained in the range 300–500 °C, suggesting a better activity of the reduced form of the noble metal. This activity was preserved in the subsequent heating cycle; however, a treatment under airflow at 800 °C restored the performance of the fresh calcined sample. This is likely related to the formation of RhO_x surface species, reducible at low temperature [16,17], and of $Rh(AlO_2)_y$ species, due to the encapsulation of Rh into alumina, reducible only at $T > 750$ °C [16] or not reducible at all [17]. CO and H_2 selectivities are in good agreement with the equilibrium ones, especially on the activated sample (Fig. 3b and c).

The presence of perovskite significantly modifies the catalytic behaviour of Rh, especially in the low temperature range (Fig. 3). Methane conversion steadily rose on both LCR_1 and LMR_1 with a steeper increase above 450 °C approaching equilibrium value from 500 °C. No hysteresis was observed for both samples upon first exposure to reaction conditions at high temperature: conversion and selectivity to syngas did not change during the cooling ramp. Moreover no carbon formation was detected. Both LCR_1 and LMR_1 catalysts are more active than fresh $Rh/\gamma\text{-}Al_2O_3$ sample at low temperature (before complete light off and total oxygen consumption). The higher conversion up to 450 °C is mainly associated to the total oxidation activity of the perovskite phase, as confirmed by the low selectivity to syngas.

At $T > 450$ °C LMR_1 and LCR_1 catalysts show CO selectivity slightly higher than that expected by equilibrium; mole fraction of CO in the downstream is over equilibrium value as well. As in the case of Rh/Al_2O_3, CO and H_2O seem to be the main products of reaction whereas the most part of H_2 is formed at higher T by secondary reactions.

For both samples, the temperature profile showed a maximum in the first part of the reactor, suggesting that O_2 is consumed at the beginning (exothermic reactions) whereas the unreacted methane is subsequently reformed with CO_2 and H_2O (endothermic reactions). The higher temperature gradients measured on LMR_1 with respect to the imposed furnace temperature (Fig. 3d) and the lower selectivity to CO and H_2 suggest that this catalyst is more active in the total oxidation of methane at low temperature, while performance of LCR_1 closely resembles that of Rh/alumina catalyst.

3.4. Pseudo-adiabatic catalytic tests

Catalytic performances of LCR_2 and LMR_2 under pseudo-adiabatic conditions as a function of CH_4/O_2 feed ratio at fixed preheating (450 °C) are reported in Fig. 4 in comparison with the results obtained with the corresponding reference Rh/Al_2O_3 catalyst. For all the three systems methane conversion follows the same trend and progressively decreases from almost 100% at $CH_4/O_2 = 1.3$ down to roughly 75% at a feed ratio of 2, in line with the qualitative trend of the adiabatic equilibrium value

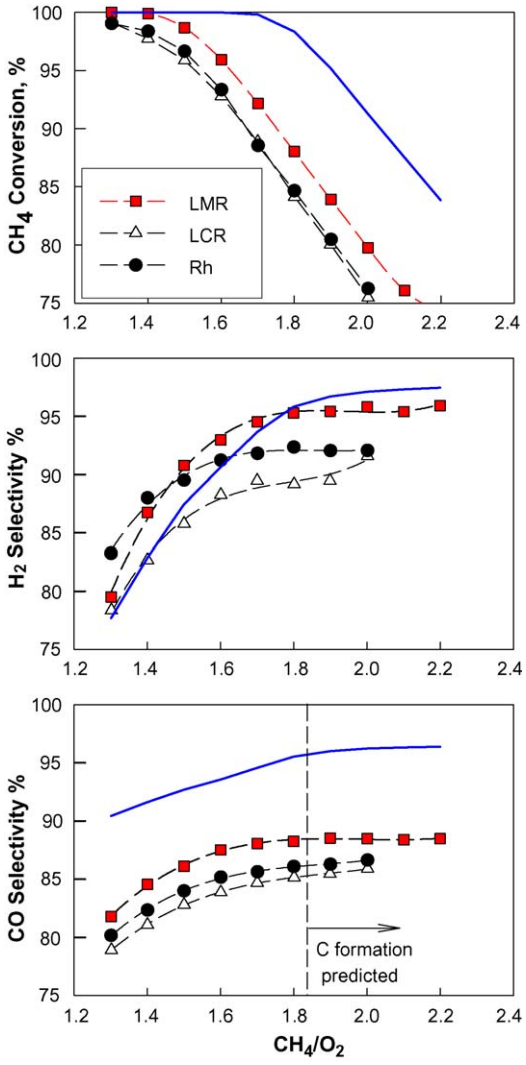

Fig. 4. CH_4 conversion, H_2 and CO selectivity under pseudo-adiabatic conditions as a function of CH_4/O_2 feed ratio over Rh/Al_2O_3 (●), LMR_2 (■) and LCR_2 (△) monoliths. Preheating 450 °C, GHSV = 36,000 h^{-1}. Solid lines correspond to equilibrium among gaseous species only.

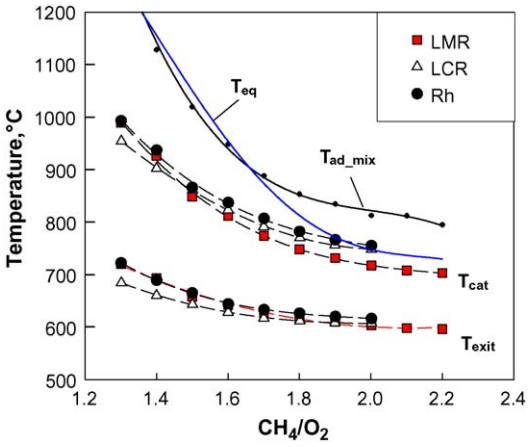

Fig. 5. Temperatures measured on catalyst surface and in the exit gas over Rh/Al_2O_3 (●), LMR_2 (■) and LCR_2 (△) monoliths as a function of CH_4/O_2 feed ratio under pseudo-adiabatic conditions. Preheating = 450 °C, GHSV = 36,000 h^{-1}. Solid lines correspond to equilibrium among gaseous species only. T_{ad_mix} is the adiabatic temperature of the exit gas mixture calculated from the experimental products distribution over LMR_2 catalyst.

calculated excluding C_s-formation. On the other hand, the formation of syngas is only slightly affected by variations in the feed composition, with H_2 and CO selectivities always exceeding 80%, which increase with CH_4/O_2 ratios up to 1.7–1.8 and then level off for richer mixtures. No carbon deposition was found, as also confirmed by the constant value of CO selectivity for CH_4/O_2 up to 2.2, while C-formation is predicted by thermodynamic equilibrium calculations for $CH_4/O_2 \geq 1.85$ (Fig. 4).

LCR_2 and Rh/Al_2O_3 catalysts showed almost identical performance in the whole range of operating conditions explored. LMR_2 catalyst performs better than LCR_2 and Rh/Al_2O_3, providing higher methane conversion and selectivity to both H_2 and CO, which in turn result in a higher syngas yield. In particular, hydrogen selectivity over LMR_2 catalyst closely follows the curve predicted by equilibrium, whereas CO is 7–8% below it for CH_4/O_2 ratios < 2, due to the formation of some CO_2 in the first part of the reactor. Therefore, the resulting syngas is characterised by a H_2/CO ratio always slightly above 2, which could be useful for downstream stabilization of a lean premixed flame, for example in the burnout zone of a gas turbine combustor, due to the high reactivity of H_2.

Fig. 5 reports the temperatures measured on the catalysts and in the exit gas leaving the reactor relevant to the experimental data presented in Fig. 4. It appears that operating temperature of the catalyst surface can be easily and directly controlled by varying the CH_4/O_2 ratio, i.e. modifying oxygen availability. Catalyst surface temperature is self-sustained in the range 700–1000 °C and progressively decreases by increasing CH_4/O_2 ratio, whereas exit gas temperature is in the range 600–700 °C and slightly decreases with the same trend of T_{cat}, indicating a rapid quench of the product mix after the catalytic monolith. In fact, the reactor operated steadily without any sign of deactivation due to overheating also at high preheating level (450 °C) and CH_4/O_2 as low as 1.3, which corresponds to an adiabatic temperature of roughly 1250 °C.

As clearly shown in Fig. 5, measured catalyst temperature resembles the adiabatic equilibrium predicted one for CH_4/O_2 down to 1.8, even if methane conversion is lower than the equilibrium value. Such behaviour is related to the catalytic total combustion of a part of the feed and further supports the hypothesis that syngas production occurs according to a reaction scheme not excluding indirect formation of H_2 and CO also under self-sustained operation. At the same time, due to heat losses by conduction and radiation from hot catalyst surface, T_{cat} is roughly 100–150 °C lower than the adiabatic temperature corresponding to the measured products distribution (T_{ad_mix} reported in Fig. 5 only for the case of LMR_2). At lower CH_4/O_2 ratios, surface temperature starts to depart more significantly from the adiabatic equilibrium value that, in turn, approaches the adiabatic temperature corresponding to the measured species in the product stream, because of the higher methane conversion. It is worth noting that, apart from the role of heat losses, the presence of a total oxidation catalyst such as the $LaMnO_3$ perovskite [13,17–20] does not appear to cause hot-spots or reactor overheating even at relatively high O_2 partial pressures. On the contrary, it was found that reactor temperatures (catalyst and exit gas) are always slightly lower over the best performing LMR_2 system, indicating a possible enhancement of the role of reforming reactions in the indirect mechanism of syngas formation.

Fig. 6 shows the main effect of increasing the GHSV at fixed preheating and feed composition is to increase both catalyst and exit gas temperatures which, in turn, entails an increase of

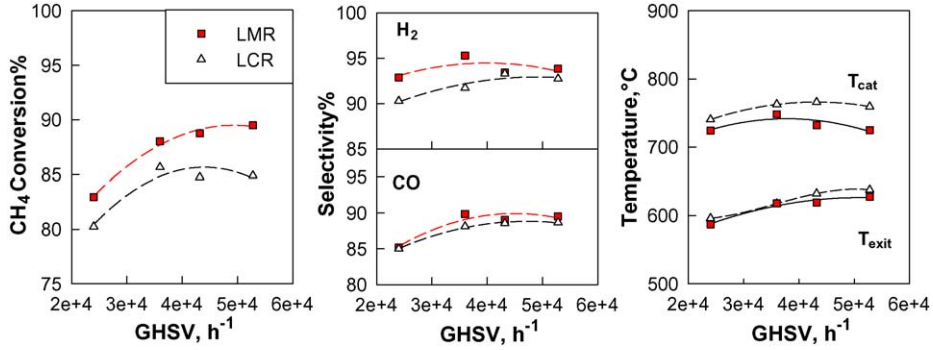

Fig. 6. CH_4 conversion, syngas selectivity and reactor temperatures over LMR_2 and LCR_2 monoliths under pseudo-adiabatic conditions as a function of GHSV. CH_4/O_2 ratio = 1.8; Preheating = 450 °C.

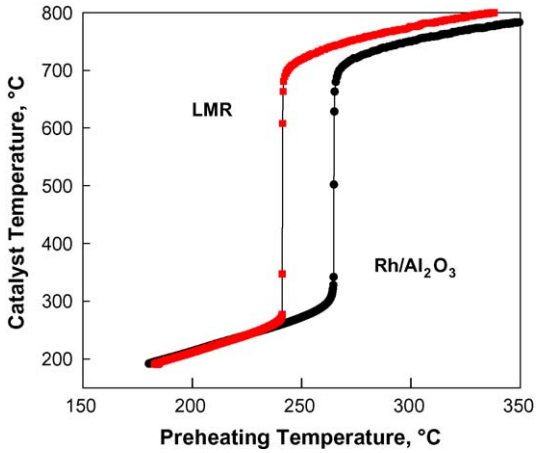

Fig. 7. Light off temperature of fuel-rich catalytic combustion over LMR_2 and Rh/Al_2O_3 monoliths under pseudo-adiabatic conditions. CH_4/O_2 ratio = 1.8; GHSV = 36,000 h^{-1}.

methane conversion and syngas selectivity, since CO and H_2 formation is favoured at higher T [7 and ref. therein]. In fact, the net increase of energy release connected to the higher feed rates of reactants can raise the temperatures in a not perfectly adiabatic system such as a lab-scale reactor, since the residence time is still long enough for the exothermal processes (transport phenomena + surface kinetics) consuming oxygen to go to completion. Fig. 6 also confirms that the better results of LMR_2 catalyst in terms of methane conversion and syngas selectivity are obtained at a lower reactor temperature in the whole range of GHSV explored.

The presence of the perovskite phase has also a positive effect for the reduction of the minimum preheating temperature required to ignite the reaction at fixed feed ratio. Fig. 7 shows that LMR_2 catalyst has a light off temperature of only 240 °C in correspondence of a feed CH_4/O_2 = 1.8, roughly 30 °C lower than the reference Rh/Al_2O_3 monolith (tested after stabilisation upon exposure to reacting conditions). This is probably due to the higher total oxidation activity displayed at low temperature by Rh–$LaMnO_3$ catalyst, which can help to reach the ignition and sustain the partial oxidation reactions by in situ heat generation and oxygen depletion.

Once ignited, the catalytic reactor can be run autothermally, i.e. the fuel-rich combustion is self-sustained even in the absence of external preheating, thus ensuring a high process flexibility. In Fig. 8 it is shown that the external preheating was varied from 500 °C down to almost room temperature over both LMR_2 and LCR_2 monoliths at fixed CH_4/O_2 ratio without causing extinction of the reaction. Methane conversion progressively decreases at lower preheating levels; CO and H_2 selectivity decrease at a lower extent, especially on LMR_2 catalyst, which still provides 90% selectivity to hydrogen without preheating, in line with the equilibrium value. It is worth noting that a large variation in the preheating temperature (450 °C) caused only a small modification of the catalyst surface temperature (roughly 50 °C), due to a self-regulation mechanism based on products redistribution and to the prevailing role of total oxidation reactions at lower temperatures.

4. Conclusions

Rh–perovskite structured catalysts are active in methane combustion under fuel-rich conditions providing high CH_4 conversion and selectivity to H_2 and CO. The addition of perovskite phase results in enhancing the activity with respect to fresh calcined Rh/Al_2O_3 catalyst with the same noble metal content, stabilizing rhodium into a more stable form which does not require pre-reduction or undergo partial activation/deactivation phenomena otherwise observed upon redox cycling at high temperature. Better performances can be obtained on LMR rather than LCR catalysts: while most Co is involved in the formation of Co-aluminate spinel, the preserved redox properties of manganese promote the occurrence of total oxidation of a fraction of methane in the first part of the monolith, thus reducing the light off temperature. Moreover Rh–$LaMnO_3$ catalyst provides higher methane conversions and syngas yields when operated under pseudo-adiabatic conditions using air as oxidant, displaying an effective synergy between the two different active sites, which seems to enhance indirect syngas formation through reforming reactions. The catalyst temperature is well controlled and self-regulated in a wide range of operating conditions (air to fuel ratio, GHSV, preheating); the presence of $LaMnO_3$ phase, promoting the total oxidation reactions, does not appear to cause hot-spot formation.

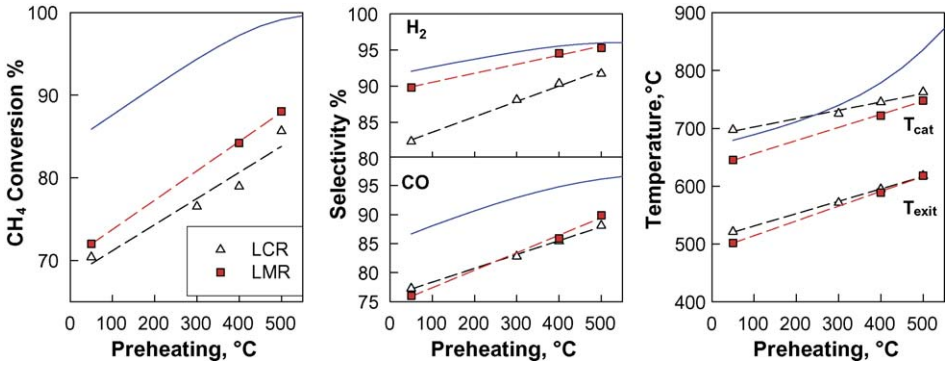

Fig. 8. CH_4 conversion, syngas selectivity and reactor temperatures over LMR_2 and LCR_2 monoliths under pseudo-adiabatic conditions as a function of preheating temperature. CH_4/O_2 ratio = 1.8; GHSV = 36,000 h^{-1}. Solid lines correspond to equilibrium among gaseous species only.

Acknowledgment

Funding from MIUR-Italy is gratefully acknowledged.

References

[1] D. Ciuparu, M. Lyubovsky, E. Altman, L. Pfefferle, A. Datye, Catal. Rev. 44 (2002) 593.
[2] M. Lyubovsky, L. Smith, M. Castaldi, H. Karim, B. Nentwick, S. Etemad, R. LaPierre, W. Pfefferle, Catal. Today 83 (2003) 71.
[3] M. Lyubovsky, S. Roychoudhury, R. LaPierre, Catal. Lett. 99 (2005) 113.
[4] L.D. Schmidt, D.A. Hickman, US Patent 5,648,582 (1997).
[5] K. Hohn, L.D. Schmidt, Appl. Catal. A 211 (2001) 53.
[6] M. Bizzi, L. Basini, G. Saracco, V. Specchia, Chem. Eng. J. 90 (2002) 97.
[7] T. Bruno, A. Beretta, G. Groppi, M. Roderi, P. Forzatti, Catal. Today 100 (2005) 89.
[8] S. Eriksson, M. Nilsson, M. Boutonnet, S. Jaras, Catal. Today 100 (2005) 447.
[9] E. Ruckentein, H.Y. Wang, J. Catal. 187 (1999) 151.
[10] L. Malocchi, G. Groppi, C. Cristiani, P. Forzatti, L. Basini, A. Guarinoni, Catal. Lett. 65 (2000) 49.
[11] S. Cimino, L. Lisi, R. Pirone, G. Russo, Ind. Eng. Chem. Res. 43 (2004) 6670.
[12] S. Cimino, F. Donsì, R. Pirone, G. Russo, D. Sanfilippo, Catal. Today 106 (2005) 72.
[13] N. Guilhaume, M. Primet, J. Catal. 165 (1997) 197.
[14] F. Basile, A. Vaccari, D. Gary, G. Fornasari, P. Del Gallo, European Patent Application EP 1419814 A1 (2004).
[15] S. Cimino, G. Landi, L. Lisi, G. Russo, Catal. Today 105 (2005) 718.
[16] W.Z. Weng, C.R. Luo, J.M.H.Q. Lin, H.L. Wan, Stud. Surf. Sci. Catal. 147 (2004) 661 (Natural Gas Conversion VII).
[17] P. Hwang, C.T. Yeh, Q. Zhu, Catal. Today 51 (1999) 93.
[18] J.L. Tejuca, J.L.G. Fierro (Eds.), Properties and Applications of Perovskite-type Oxides, Marcel Dekker, New York, 1993.
[19] L. Lisi, G. Bagnasco, P. Ciambelli, S. De Rossi, P. Porta, G. Russo, M. Turco, J. Solid State Chem. 146 (1999) 176.
[20] S. Cimino, L. Lisi, S. De Rossi, M. Faticanti, P. Porta, Appl. Catal. B 43 (2003) 397.
[21] S. Cimino, S. Colonna, S. De Rossi, M. Faticanti, L. Lisi, I. Pettiti, P. Porta, J. Catal. 205 (2002) 309.
[22] O. Dulaurent, K. Chandes, C. Bouly, D. Bianchi, J. Catal. 192 (2000) 262.
[23] F. Solymosi, M. Pásztor, J. Catal. 104 (1987) 312.
[24] R.J. Kee, F.M. Rupley, J.A. Miller, M.E. Coltrin, J.F. Grcar, E. Meeks, H.K. Moffat, A.E. Lutz, G. Dixon-Lewis, M.D. Smooke, J. Warnatz, G.H. Evans, R.S. Larson, R.E. Mitchell, L.R. Petzold, W.C. Reynolds, M. Caracotsios, W.E. Stewart, P. Glarborg, C. Wang, O. Adigun, Chemkin Collection Release 4.0, Reaction Design, Inc., San Diego, CA, 2004.